

ON THE ERROR ESTIMATES FOR THE ROTATIONAL PRESSURE-CORRECTION PROJECTION SPECTRAL METHODS FOR THE UNSTEADY STOKES EQUATIONS ^{*1)}

Feng-hui Huang Chuan-ju Xu

(*Department of Mathematics, Xiamen University, Xiamen 361005, China*)

Abstract

This paper provides an analysis of the rotational form of the pressure-correction methods by spectral approximations for the unsteady Stokes equations. Error estimates in finite time for the fully discrete case are given. Numerical experiences using both spectral and spectral element methods are carried out to confirm the theoretical results.

Mathematics subject classification: 76M22, 76D05, 65M12, 65M70.

Key words: Stokes equations, Projection methods, Spectral methods.

1. Introduction

Efficient solution of the Stokes equations is dependent upon the availability of fast solvers for the pressure operator, as the pressure characteristic propagation speed is infinite for unsteady incompressible flow. Generally, there are two principal ways to discretize the unsteady Stokes equations in time. One way is to keep the velocity and the pressure coupled, and at each time step it needs to solve the generalized Stokes problem which is the most computationally expensive. A common technique for solving the algebraic system, stemming from discretization of the Stokes equations, is the Uzawa algorithm. An Uzawa algorithm uses block Gaussian elimination and back substitution for the pressure and the velocity yielding two positive definite symmetric systems (see e.g. [19] and the references therein). This decoupling procedure has been proven to be attractive than a direct algorithm. However the classical Uzawa algorithm suffers from expensive solve of the pressure system as the pressure matrix involves the inverses of the Helmholtz systems. This disadvantage could be overcome by using an additional splitting technique. This approach has a common foundation with traditional splitting approaches which leads to a Poisson equation for the pressure except that, in the former case, the splitting is effected in the discrete form of the equations. Such an approach was analyzed and applied to the various computations in the papers of Perot [21], Couzy *et al.* [9] and Fischer [11], but no rigorous error estimate is available. The disadvantage of the Uzawa-based algorithm is that a discrete form of the Ladyshenskaya-Brezzi-Babuška condition (LBB condition, [5]) must be satisfied for obtaining the unique discrete solution. This means that for a high-order spectral approximation, the degree of approximation for the pressure must be taken two degrees lower than that for the velocity [20]. It is the so called $P_N \times P_{N-2}$ method. There exist some methods that make use other space pairs than $P_N \times P_{N-2}$, we refer to [6] for detailed description of these methods.

Another way to discretize the continuous unsteady Stokes equations is provided by the class of projection methods. This class of approaches has been introduced by Chorin [7, 8] and Temam [28]. They are based on a particular time-discretization of the equations governing

* Received December 12, 2003; final revised August 23, 2004.

¹⁾ This work was supported by National NSF of China under Grant 10171084 and the Excellent Young Teachers Program (EYTP) of MOE of China.

viscous incompressible flows, in which the viscosity and the incompressibility of the fluid are dealt within two separate steps. By doing that, the original problem is reformulated into two new and simpler problems. The theory of saddle-point problems is then no longer needed, that is to say, the LBB condition is not needed; as a consequence, the degree of approximation for the velocity and the pressure can be taken the same, yielding a simpler-to-implement numerical scheme.

The projection algorithm can be interpreted as a predictor-corrector strategy, which can be essentially classed into two families: classical fractional step methods and pressure-correction methods. The classical fractional step methods have only first order convergence rate due to the fact that it is basically an artificial compressibility technique [24, 25]. Different choices of the pressure boundary condition have been discussed to improve the efficiency of this kind of methods (see [17] for instance). The pressure-correction methods consist of two time substeps: first we make the pressure explicit in the convection-diffusion step, and then compute its increment (correction) in the projection step. Second-order Error estimates in the L^2 -norm for the velocity have been proved in the several papers [10, 26, 15, 27] for different cases. However the pressure accuracy in a standard pressure-correction scheme can be at most of first-order in the L^2 -norm, as shown by Strikwerda and Lee in [27]. In 1996, Timmermans, Minnev and Van De Vosse introduced in [30] a modified pressure-correction scheme. They analyzed this approach by means of an analytical test solution in the case of spectral element spatial discretization, and showed that the L^2 errors of both the velocity and the gradient of the pressure are of second-order, but the computed maximum pressure failed to converge due to the presence of the corners. Recently, Guermond and Shen [14] reviewed this modified version of the pressure-correction schemes. They termed it as the *rotational form* of the pressure-correction schemes, and showed that the pressure approximation in the L^2 -norm is indeed $\frac{3}{2}$ -order accurate. A detail proof was given in the semi-discrete case.

The main task of the present paper is to provide a rigorous stability and error analysis for the rotational form of the pressure-correction schemes in the fully discrete case using a Galerkin spectral approximation. In order to get the optimal error estimates, we still assume that the approximate velocity and pressure space pair satisfies the LBB condition. We prove that the velocity error in time and in space is $O(\delta t^2 + N^{-m})$ for the $l^2(L^2(\Omega)^2)$ -norm and that the pressure error is $O(\delta t^{\frac{3}{2}} + N^{-m})$ for the $l^2(L^2(\Omega))$ -norm, where N is the polynomial degree used to approximate the velocity, δt is the time step, m is the regularity of the exact pressure solution. Our numerical experiences are in good agreement with the above theoretical results for the velocity, but the computed pressure appears to have higher order accuracy in time than $O(\delta t^{\frac{3}{2}})$. Particularly our numerical results show that the pressure accuracy is sensible to the kinematics viscosity in the case of singular computational domain. In the case of square domain, for the $L^2(\Omega)$ norm at a given time $T \geq 1$, the pressure accuracy is less than 2-order. But in the case of smooth domain, the pressure accuracy is fully 2-order. This conforms to the results given in [30] and [14].

We should emphasize that, in order to gain maximal simplicity in the implementation, our numerical experiences use spectral and spectral element approximations of $P_N \times P_N$ version (we refer to [14] for the $P_N \times P_{N-2}$ version). As already indicated in [14], there are larger pressure errors at the domain corners for the projection $P_N \times P_{N-2}$ spectral methods. Our numerical results show that these larger pressure errors will be further enlarged if the $P_N \times P_N$ version is used, and the maximum pressure error fails to converge due to the presence of the corners, specially for very small δt . However we will show that this failure can be efficiently overcome by a simple filtering procedure, which consists in projecting the computed pressure into P_{N-2} space at each time step. This procedure is, in some sense, equivalent to the $P_N \times P_{N-2}$ version, but is easier to implement. We refer it to as the filtered $P_N \times P_N$ version.

The outline of this paper is as follow: in Section 2 we recall the basic steps of projection-type methods, and define their spectral approximation formulations. In section 3 we provide rigorous

error estimations to the fully discrete rotational projection spectral methods. Numerical tests are given in Section 4. Finally we give some concluding remarks in section 5.

2. Rotational Projection Spectral Methods for the Unsteady Stokes Problem

2.1 Notations and hypotheses

Let Ω be an open connected bounded domain of \mathbb{R}^2 with a piecewise smooth boundary $\partial\Omega$. More specifically, the domain must be piecewise smooth enough so that Cattabriga's regularity estimates for the Stokes problem hold [29]. In this paper, $W^{s,p}(\Omega)$ denotes the real Sobolev spaces, $0 \leq s \leq \infty, 0 \leq p \leq \infty$, equipped with the norm $\|\cdot\|_{s,p}$. The completion with respect to the $\|\cdot\|_{s,p}$ norm of the space of the smooth functions compactly supported in Ω is denoted by $W_0^{s,p}(\Omega)$. The Hilbert spaces $W^{s,2}(\Omega)$ is denoted by $H^s(\Omega)$, the related norm is denoted by $\|\cdot\|_s$. In particular, the norm and inner product of $L^2(\Omega)$, *i.e.* $H^0(\Omega)$, are denoted by $\|\cdot\|$ and (\cdot, \cdot) respectively. We also introduce the following Hilbert spaces:

$$\begin{aligned} X &= H_0^1(\Omega)^2 = \{v \in H^1(\Omega)^2, v|_{\partial\Omega} = 0\}, \quad V = \{v \in X, \nabla \cdot v = 0\}, \\ L_0^2(\Omega) &= \{q \in L^2(\Omega), \int_{\Omega} q = 0\}, \quad M = L_0^2(\Omega) \cap H^1(\Omega), \\ X_N &= X \cap P_N(\Omega)^2, \quad M_N = M \cap P_{N-2}(\Omega), \quad Y_N = P_N(\Omega)^2, \\ H_N &= \{v_N \in Y_N; (v_N, \nabla q_N) = 0, \forall q_N \in M_N\}, \\ V_N &= \{v_N \in X_N; (\nabla \cdot v_N, q_N) = (v_N, \nabla q_N) = 0, \forall q_N \in M_N\}. \end{aligned}$$

where $P_N(\Omega)$ is the space of polynomials of degree less or equal than N with respect to each variable in Ω . It is known [20] that the space pair $X_N \times M_N$ satisfies the LBB condition:

$$\inf_{q_N \in M_N} \sup_{v_N \in X_N} \frac{-(\nabla \cdot v_N, q_N)}{\|v_N\|_1 \|q_N\|} \geq \beta_N > 0, \quad (1)$$

where $\beta_N \sim N^{-1/2}$.

The following projection operators are useful for the error estimations:

$P_{H_N} : Y_N \rightarrow H_N$ as the L^2 -orthogonal projector is defined by: given $\varphi_N \in Y_N, P_{H_N} \varphi_N \in H_N$, s.t.

$$(\varphi_N - P_{H_N} \varphi_N, \psi_N) = 0, \quad \forall \psi_N \in H_N.$$

$\Pi_N : L^2(\Omega) \rightarrow M_N$ as the L^2 -orthogonal projector is defined by: given $\varphi \in L^2(\Omega), \Pi_N \varphi \in M_N$, s.t.

$$(\varphi - \Pi_N \varphi, \psi_N) = 0, \quad \forall \psi_N \in M_N.$$

$\Pi_N^0 : V \rightarrow V \cap P_N(\Omega)^2$ as the norm $\|\cdot\|_1$ orthogonal projector is defined by: given $\varphi \in V, \Pi_N^0 \varphi \in V \cap P_N(\Omega)^2$, s.t.

$$(\nabla(\varphi - \Pi_N^0 \varphi), \nabla \psi_N) = 0, \quad \forall \psi_N \in V \cap P_N(\Omega)^2.$$

$\Pi_N^1 : H^1(\Omega) \rightarrow M_N$ as the norm $\|\cdot\|_1$ orthogonal projector is defined by: given $\varphi \in H^1(\Omega), \Pi_N^1 \varphi \in M_N$, s.t.

$$\left(\nabla(\varphi - \Pi_N^1 \varphi), \nabla \psi_N \right) + (\varphi - \Pi_N^1 \varphi, \psi_N) = 0, \quad \forall \psi_N \in M_N.$$

Then we have the following properties

$$\begin{aligned} \|P_{H_N} \varphi_N\| &\leq \|\varphi_N\|, \quad \forall \varphi_N \in Y_N; \\ \|\Pi_N \varphi\| &\leq \|\varphi\|, \quad \forall \varphi \in L^2(\Omega); \\ \|\Pi_N^1 \varphi\|_1 &\leq \|\varphi\|_1, \quad \forall \varphi \in H^1(\Omega); \end{aligned}$$

$$\begin{aligned}
 |\varphi - \Pi_N^0 \varphi|_1 + N \|\varphi - \Pi_N^0 \varphi\| &\leq cN^{-m} \|\varphi\|_{m+1}, \quad \forall \varphi \in V; \\
 |\varphi - \Pi_N^1 \varphi|_1 + N \|\varphi - \Pi_N^1 \varphi\| &\leq cN^{-m} \|\varphi\|_{m+1}, \quad \forall \varphi \in H^1(\Omega),
 \end{aligned}$$

where and hereafter in this section, c denotes a generic positive constant.

Finally, we introduce the discrete inverse Stokes operator $S_N : Y_N \rightarrow V_N$: for all $v_N \in Y_N, (S_N v_N, r_N) \in X_N \times M_N$ is the solution of the following problem

$$\begin{cases} (\nabla S_N v_N, \nabla w_N) - (\nabla \cdot w_N, r_N) = (v_N, w_N), & \forall w_N \in X_N, \\ (\nabla \cdot S_N v_N, q_N) = 0, & \forall q_N \in M_N. \end{cases} \tag{2}$$

Note that the second equation of (2) means $S_N v_N \in V_N$, therefore the operator S_N is well defined. We assume that $\partial\Omega$ is sufficiently piecewise smooth such that the following stability property holds:

$$\|\nabla r_N\| \leq c \|v_N\|, \quad \forall v_N \in Y_N. \tag{3}$$

Remark 2.1. It is known that the stability property (3) holds in the frame of finite element methods(see e.g. [15]). In the frame of spectral methods, this stability assumption has not been proven theoretically. However, (3) has been verified by a number of numerical experiences.

The following symmetry can be easily obtained from (2)

$$(\varphi_N, S_N \psi_N) = (\nabla S_N \varphi_N, \nabla S_N \psi_N) = (\psi_N, S_N \varphi_N), \quad \forall \varphi_N, \psi_N \in Y_N. \tag{4}$$

Lemma 2.1. *The linear form $v_N \mapsto (v_N, S_N v_N)^{1/2}$ for $v_N \in Y_N$ induces a semi-norm on V_N , which we denote by $\|v_N\|_\star = (v_N, S_N v_N)^{1/2}$. Then we have $|S_N v_N|_1 = \|v_N\|_\star$, and*

$$\|S_N v_N\|_1 \leq c \|v_N\|_\star \leq c \|v_N\|_{-1}. \tag{5}$$

Lemma 2.2. *For all $v_N \in H_N, w_N \in X_N$, we have*

$$(\nabla S_N v_N, \nabla w_N) \geq (P_{H_N} w_N, v_N) - c \|v_N\| \|w_N - P_{H_N} w_N\|. \tag{6}$$

Furthermore, for all $0 < \alpha < 1$, the following properties of S_N hold

$$(\nabla S_N w_N, \nabla w_N) \geq (1 - \alpha) \|w_N\|^2 - c_\alpha \|w_N - P_{H_N} w_N\|^2, \tag{7}$$

$$(\nabla S_N P_{H_N} w_N, \nabla w_N) \geq (1 - \alpha) \|P_{H_N} w_N\|^2 - c_\alpha \|w_N - P_{H_N} w_N\|^2. \tag{8}$$

Proof. Using (2) and (3), we have

$$\begin{aligned}
 (\nabla S_N v_N, \nabla w_N) &= (v_N, w_N) + (\nabla \cdot w_N, r_N) \\
 &= (v_N, w_N) - (w_N, \nabla r_N) \\
 &= (P_{H_N} w_N, v_N) - (w_N - P_{H_N} w_N, \nabla r_N) \\
 &\geq (P_{H_N} w_N, v_N) - \|w_N - P_{H_N} w_N\| \|\nabla r_N\| \\
 &\geq (P_{H_N} w_N, v_N) - c \|v_N\| \|w_N - P_{H_N} w_N\|,
 \end{aligned}$$

which gives (6). Taking $v_N = P_{H_N} w_N$ in (6) and using the Young inequality, we obtain (8). Finally, let $v_N = w_N$ in (2), then

$$\begin{aligned}
 (\nabla S_N w_N, \nabla w_N) &= (w_N, w_N) + (\nabla \cdot w_N, r_N) \\
 &= (w_N, w_N) - (w_N, \nabla r_N) \\
 &= \|w_N\|^2 - (w_N - P_{H_N} w_N, \nabla r_N) \\
 &\geq \|w_N\|^2 - \|w_N - P_{H_N} w_N\| \|\nabla r_N\| \\
 &\geq \|w_N\|^2 - c \|w_N\| \|w_N - P_{H_N} w_N\| \\
 &\geq (1 - \alpha) \|w_N\|^2 - c_\alpha \|w_N - P_{H_N} w_N\|^2,
 \end{aligned}$$

it is the result (7).

2.2 The rotational pressure-correction projection scheme

We consider the following time-dependent Stokes equations in which homogeneous Dirichlet condition has been assumed for simplicity. For a given body force f (possibly dependent on time) and a given divergence-free initial velocity field u_0 , find a velocity field u and a pressure field p so that at $t = 0, u = u_0$, and at all subsequent time

$$\begin{cases} \frac{\partial u}{\partial t} - \nu \nabla^2 u + \nabla p = f, & \text{in } \Omega \times (0, T], \\ \nabla \cdot u = 0, & \text{in } \Omega \times (0, T], \\ u = 0, & \text{in } \partial\Omega \times (0, T]. \end{cases} \quad (9)$$

We now recall the pressure-correction algorithm using *BF2* [14] to march in time for solving the problem (9). The first sub-step accounting for viscous diffusion is

$$\begin{cases} \frac{3\tilde{u}^{k+1} - 4u^k + u^{k-1}}{2\delta t} - \nu \nabla^2 \tilde{u}^{k+1} + \nabla p^k = f(t^{k+1}), \\ \tilde{u}^{k+1}|_{\partial\Omega} = 0, \end{cases} \quad (10)$$

and the second sub-step accounting for incompressibility is

$$\begin{cases} \frac{3u^{k+1} - 3\tilde{u}^{k+1}}{2\delta t} - \nabla(p^{k+1} - p^k) = 0, \\ \nabla \cdot u^{k+1} = 0, \\ u^{k+1} \cdot \mathbf{n}|_{\partial\Omega} = 0. \end{cases} \quad (11)$$

This method is called as the pressure-correction scheme in standard form. Though it is second order accurate on the velocity in the L^2 -norm, it is plagued by a numerical boundary layer that prevent it to be fully second order in the H^1 -norm of the velocity and in the L^2 -norm of the pressure. A modified scheme with a divergence correction has been proposed in [30], which was then called in [14] as the pressure-correction scheme in rotational form. In this scheme the second step (11) is replaced by

$$\begin{cases} \frac{3u^{k+1} - 3\tilde{u}^{k+1}}{2\delta t} + \nabla(p^{k+1} - p^k + \nu \nabla \cdot \tilde{u}^{k+1}) = 0, \\ \nabla \cdot u^{k+1} = 0, \\ u^{k+1} \cdot \mathbf{n}|_{\partial\Omega} = 0. \end{cases} \quad (12)$$

Numerical experiences have shown that the scheme in rotational form (10) and (12) provides better approximations for the pressure. This scheme was reviewed by Guermond and Shen, who gave a detailed error analysis in its semi-discrete form [14].

2.3 Full discretization

Now we consider the full discretization of the scheme in rotational form (10) and (12). For a fixed finite time $T > 0$, we introduce a partition of the time interval $[0, T]$, $t^k = k\delta t$ for $0 \leq k \leq K$, where $\delta t = T/K$. We are interested in defining a fully discrete rotational form of the pressure-correction algorithm for $k \leq K$; and define two sequences of approximate velocities $\tilde{u}_N^k \in X_N$, $u_N^k \in Y_N$ and one sequence of approximate pressures $p_N^k \in M_N$ such that

$$\begin{aligned} & \left(\frac{3\tilde{u}_N^{k+1} - 4u_N^k + u_N^{k-1}}{2\delta t}, v_N \right) + \nu (\nabla \tilde{u}_N^{k+1}, \nabla v_N) - (p_N^k, \nabla \cdot v_N) \\ & = (f^{k+1}, v_N), \quad \forall v_N \in X_N, \end{aligned} \quad (13)$$

and

$$\begin{cases} \left(\frac{3u_N^{k+1} - 3\tilde{u}_N^{k+1}}{2\delta t}, v_N \right) + \left(\nabla(p_N^{k+1} - p_N^k + \nu \Pi_N \nabla \cdot \tilde{u}_N^{k+1}), v_N \right) = 0, & \forall v_N \in Y_N, \\ (u_N^{k+1}, \nabla q_N) = 0, & \forall q_N \in M_N. \end{cases} \quad (14)$$

The step (14) is a realization of the projection $u_N^{k+1} = P_{H_N} \tilde{u}_N^{k+1}$. In the implementation, we take $v_N = \nabla q_N$ in the first equation of (14), so that we can obtain a discrete Poisson equation for the pressure increment $p_N^{k+1} - p_N^k + \nu \Pi_N \nabla \cdot \tilde{u}_N^{k+1}$.

3. The Error Analysis

3.1 Preliminaries

Before going through the details of the error analysis, we introduce some technical tools. For any sequence $w = \{w^0, w^1, \dots, w^K\}$ in Sobolev space W , w is equipped with norm

$$\|w\|_{l^2(W)} = \left(\delta t \sum_{k=0}^K \|w^k\|_W^2\right)^{1/2}.$$

We set

$$\begin{aligned} \delta_t w^k &= w^k - w^{k-1}, & \delta_{tt} w^k &= \delta_t(\delta_t w^k), \\ \delta_{ttt} w^k &= \delta_t(\delta_{tt} w^k), & D_t w^{k+1} &= \frac{3w^{k+1} - 4w^k + w^{k-1}}{2}. \end{aligned}$$

We can easily derive the following useful algebraic identities:

$$2(w^{k+1}, w^{k+1} - w^k) = |w^{k+1}|^2 + |w^{k+1} - w^k|^2 - |w^k|^2, \quad (15)$$

$$\begin{aligned} &2(w^{k+1}, 3w^{k+1} - 4w^k + w^{k-1}) \\ &= |w^{k+1}|^2 + |2w^{k+1} - w^k|^2 + |\delta_{tt} w^{k+1}|^2 - |w^k|^2 - |2w^k - w^{k-1}|^2. \end{aligned} \quad (16)$$

We denote $u^k = u(t^k)$, $p^k = p(t^k)$, and

$$\begin{aligned} e_N^k &= u_N^k - \Pi_N^0 u^k, & \tilde{e}_N^k &= \tilde{u}_N^k - \Pi_N^0 u^k, \\ \varepsilon_N^k &= p_N^k - \Pi_N^1 p^k, & \psi_N^k &= p_N^k - \Pi_N^1 p^{k+1}. \end{aligned} \quad (17)$$

3.2 Error estimations

We assume that the couple exact solution (u, p) of the Stokes equations (9) is smooth enough in time and in space. For simplicity we set $\nu = 1$ and assume that the projection algorithm is initialized so that

$$\max(\|e_N^0\|, \|e_N^1\|, \|\tilde{e}_N^0\|_1, \|\tilde{e}_N^1\|_1) \leq c\delta t^2, \quad \max(\|\varepsilon_N^0\|, \|\varepsilon_N^1\|) \leq c, \quad (18)$$

where and hereafter in this paper, c denotes a generic positive constant, which may depend on the couple exact solution.

Lemma 3.1. *Under the initial hypotheses (18), for all $1 \leq n \leq K$, we have the following estimates,*

$$\sum_{k=1}^n \|\delta_t e_N^{k+1} - \delta_t \tilde{e}_N^{k+1}\|^2 \leq c\delta t^2 (\delta t^2 + N^{-2m}), \quad (19)$$

$$\|\Pi_N \nabla \cdot \tilde{e}_N^{n+1}\| \leq c\delta t^{1/2} (\delta t + N^{-m}), \quad (20)$$

$$\|e_N^{n+1} - \tilde{e}_N^{n+1}\| \leq c\delta t (\delta t + N^{-m}). \quad (21)$$

Proof. Step 1. The solution of problem (9) satisfies at time t^{k+1}

$$\begin{cases} (u_t^{k+1}, v_N) + (\nabla u^{k+1}, \nabla v_N) - (\nabla \cdot v_N, p^{k+1}) = (f^{k+1}, v_N), & \forall v_N \in X_N, \\ (\nabla \cdot u^{k+1}, q_N) = 0, & \forall q_N \in M_N. \end{cases} \quad (22)$$

Then we have

$$\begin{cases} \left(\frac{3\Pi_N^0 u^{k+1} - 4\Pi_N^0 u^k + \Pi_N^0 u^{k-1}}{2\delta t}, v_N \right) + (\nabla \Pi_N^0 u^{k+1}, \nabla v_N) - (\Pi_N^1 p^{k+1}, \nabla \cdot v_N) \\ = (f^{k+1} - R^{k+1}, v_N) - (Q^{k+1}, \nabla \cdot v_N), & \forall v_N \in X_N, \\ (\nabla \cdot \Pi_N^0 u^{k+1}, q_N) = -(\Pi_N^0 u^{k+1}, \nabla q_N) = 0, & \forall q_N \in M_N, \end{cases} \quad (23)$$

where R^{k+1} and Q^{k+1} are defined by

$$R^{k+1} = u_t^{k+1} - \frac{3\Pi_N^0 u^{k+1} - 4\Pi_N^0 u^k + \Pi_N^0 u^{k-1}}{2\delta t},$$

$$Q^{k+1} = \Pi_N^1 p^{k+1} - p^{k+1},$$

which can be controlled by

$$\|R^{k+1}\| \leq c(\delta t^2 + N^{-(m+1)}),$$

and

$$\|Q^{k+1}\| \leq cN^{-m}.$$

By subtracting the equation (13) from (23), and adding null terms $\Pi_N^0 u^{k+1} - \Pi_N^0 u^{k+1}$, $\Pi_N^1 p^{k+1} - \Pi_N^1 p^{k+1} - \Pi_N(\nabla \cdot \Pi_N^0 u^{k+1})$ to (14), we derive the equations that control the errors

$$\begin{aligned} & \left(\frac{3\tilde{e}_N^{k+1} - 4e_N^k + e_N^{k-1}}{2\delta t}, v_N \right) + (\nabla \tilde{e}_N^{k+1}, \nabla v_N) - (\psi_N^k, \nabla \cdot v_N) \\ & = (R^{k+1}, v_N) + (Q^{k+1}, \nabla \cdot v_N), \quad \forall v_N \in X_N, \end{aligned} \quad (24)$$

and

$$\begin{cases} \left(\frac{3\tilde{e}_N^{k+1} - 3\tilde{e}_N^{k+1}}{2\delta t}, v_N \right) + (\nabla(\tilde{e}_N^{k+1} - \psi_N^k + \Pi_N \nabla \cdot \tilde{e}_N^{k+1}), v_N) = 0, & \forall v_N \in Y_N, \\ (e_N^{k+1}, \nabla q_N) = 0, & \forall q_N \in M_N. \end{cases} \quad (25)$$

Furthermore, we can derive the equations that control the time increments of the errors

$$\begin{aligned} & \left(\frac{3\delta_t \tilde{e}_N^{k+1} - 4\delta_t e_N^k + \delta_t e_N^{k-1}}{2\delta t}, v_N \right) + (\nabla \delta_t \tilde{e}_N^{k+1}, \nabla v_N) + (\nabla \delta_t \psi_N^k, v_N) \\ & = (\delta_t R^{k+1}, v_N) + (\delta_t Q^{k+1}, \nabla \cdot v_N), \quad \forall v_N \in X_N, \end{aligned} \quad (26)$$

and

$$\begin{cases} \frac{3}{2\delta t}(\delta_t e_N^{k+1}, v_N) + (\nabla(\delta_t \tilde{e}_N^{k+1} + \Pi_N \nabla \cdot \tilde{e}_N^{k+1}), v_N) \\ = \frac{3}{2\delta t}(\delta_t \tilde{e}_N^{k+1}, v_N) + (\nabla(\delta_t \psi_N^k + \Pi_N \nabla \cdot \tilde{e}_N^k), v_N), & \forall v_N \in Y_N, \\ (\delta_t e_N^{k+1}, \nabla q_N) = 0, & \forall q_N \in M_N. \end{cases} \quad (27)$$

Step 2. We take $v_N = 4\delta t \delta_t \tilde{e}_N^{k+1} \in X_N$ in (26) to get

$$\begin{aligned} & 2(\delta_t \tilde{e}_N^{k+1}, 3\delta_t \tilde{e}_N^{k+1} - 4\delta_t e_N^k + \delta_t e_N^{k-1}) + 4\delta t(\nabla \delta_t \tilde{e}_N^{k+1}, \nabla \delta_t \tilde{e}_N^{k+1}) + 4\delta t(\delta_t \tilde{e}_N^{k+1}, \nabla \delta_t \psi_N^k) \\ & = 4\delta t(\delta_t \tilde{e}_N^{k+1}, \delta_t R^{k+1}) + 4\delta t(\nabla \cdot \delta_t \tilde{e}_N^{k+1}, \delta_t Q^{k+1}). \end{aligned}$$

We use a technique similar to that used in [14] to treat the first term which is denoted by I , then

$$\begin{aligned} I = & 6(\delta_t \tilde{e}_N^{k+1}, \delta_t \tilde{e}_N^{k+1} - \delta_t e_N^{k+1}) + 2(\delta_t e_N^{k+1}, 3\delta_t e_N^{k+1} - 4\delta_t e_N^k + \delta_t e_N^{k-1}) \\ & + 2(\delta_t \tilde{e}_N^{k+1} - \delta_t e_N^{k+1}, 3\delta_t e_N^{k+1} - 4\delta_t e_N^k + \delta_t e_N^{k-1}). \end{aligned} \quad (28)$$

Applying the identities (15)-(16) to the first two terms of (28), which are denoted by I_1 and I_2 respectively, leads to

$$\begin{aligned} I_1 & = 3\|\delta_t \tilde{e}_N^{k+1}\|^2 + 3\|\delta_t e_N^{k+1} - \delta_t \tilde{e}_N^{k+1}\|^2 - 3\|\delta_t e_N^{k+1}\|^2, \\ I_2 & = \|\delta_t e_N^{k+1}\|^2 + \|2\delta_t e_N^{k+1} - \delta_t e_N^k\|^2 + \|\delta_{ttt} e_N^{k+1}\|^2 - \|\delta_t e_N^k\|^2 - \|2\delta_t e_N^k - \delta_t e_N^{k-1}\|^2. \end{aligned}$$

Noting the fact that $3\delta_t e_N^{k+1} - 4\delta_t e_N^k + \delta_t e_N^{k-1}$ belongs to H_N and owing to (27), we find that the last term I_3 of (28) is vanishing:

$$\frac{3}{2\delta t} I_3 = 2\left(\nabla \delta_t(\tilde{e}_N^{k+1} - \psi_N^k) + \nabla(\Pi_N(\nabla \cdot \delta_t \tilde{e}_N^{k+1})), 3\delta_t e_N^{k+1} - 4\delta_t e_N^k + \delta_t e_N^{k-1} \right) = 0.$$

Combining all above results, we have

$$\begin{aligned} & 3\|\delta_t \tilde{e}_N^{k+1}\|^2 - 3\|\delta_t e_N^{k+1}\|^2 + 3\|\delta_t e_N^{k+1} - \delta_t \tilde{e}_N^{k+1}\|^2 + \|\delta_t e_N^{k+1}\|^2 + \|2\delta_t e_N^{k+1} - \delta_t e_N^k\|^2 \\ & - \|\delta_t e_N^k\|^2 - \|2\delta_t e_N^k - \delta_t e_N^{k-1}\|^2 + \|\delta_{ttt} e_N^{k+1}\|^2 + 4\delta t\|\nabla \delta_t \tilde{e}_N^{k+1}\|^2 + 4\delta t(\delta_t \tilde{e}_N^{k+1}, \nabla \delta_t \psi_N^k) \\ & = 4\delta t(\delta_t \tilde{e}_N^{k+1}, \delta_t R^{k+1}) + 4\delta t(\nabla \cdot \delta_t \tilde{e}_N^{k+1}, \delta_t Q^{k+1}) \\ & \leq c_1 \delta t \|\delta_t \tilde{e}_N^{k+1}\|^2 + c(c_1) \delta t \|\delta_t R^{k+1}\|^2 + c_2 \delta t \|\nabla \cdot \delta_t \tilde{e}_N^{k+1}\|^2 + c(c_2) \delta t \|\delta_t Q^{k+1}\|^2 \\ & \leq c_1 \tilde{c} \delta t \|\nabla \delta_t \tilde{e}_N^{k+1}\|^2 + c_2 \delta t \|\nabla \cdot \delta_t \tilde{e}_N^{k+1}\|^2 + c \delta t \|\delta_t R^{k+1}\|^2 + c \delta t \|\delta_t Q^{k+1}\|^2. \end{aligned} \quad (29)$$

Where \tilde{c} is a constant such that $\|v\|^2 \leq \tilde{c}\|\nabla v\|^2$ and the positive constants c_1, c_2 will be determined in the later.

Step 3. By taking v_N in (27) to be $2\delta t\delta_t e_N^{k+1}, 2\delta t\delta_t \tilde{e}_N^{k+1}, \frac{4\delta t^2}{3}\nabla(\delta_t \varepsilon_N^{k+1} + \Pi_N \nabla \cdot \tilde{e}_N^{k+1}), \frac{4\delta t^2}{3}\nabla(\delta_t \psi_N^k + \Pi_N \nabla \cdot \tilde{e}_N^k)$ respectively, and using the second equation of (27), we obtain the following equalities:

$$\begin{aligned} & 3\|\delta_t e_N^{k+1}\|^2 = 3(\delta_t \tilde{e}_N^{k+1}, \delta_t e_N^{k+1}), \\ & 3(\delta_t e_N^{k+1}, \delta_t \tilde{e}_N^{k+1}) + 2\delta t \left(\delta_t \tilde{e}_N^{k+1}, \nabla(\delta_t \varepsilon_N^{k+1} + \Pi_N \nabla \cdot \tilde{e}_N^{k+1}) \right) \\ & = 3\|\delta_t \tilde{e}_N^{k+1}\|^2 + 2\delta t \left(\delta_t \tilde{e}_N^{k+1}, \nabla(\delta_t \psi_N^k + \Pi_N \nabla \cdot \tilde{e}_N^k) \right), \\ & \frac{4\delta t^2}{3} \|\nabla(\delta_t \varepsilon_N^{k+1} + \Pi_N \nabla \cdot \tilde{e}_N^{k+1})\|^2 \\ & = 2\delta t \left(\delta_t \tilde{e}_N^{k+1}, \nabla(\delta_t \varepsilon_N^{k+1} + \Pi_N \nabla \cdot \tilde{e}_N^{k+1}) \right) \\ & \quad + \frac{4\delta t^2}{3} \left(\nabla(\delta_t \varepsilon_N^{k+1} + \Pi_N \nabla \cdot \tilde{e}_N^{k+1}), \nabla(\delta_t \psi_N^k + \Pi_N \nabla \cdot \tilde{e}_N^k) \right), \\ & \frac{4\delta t^2}{3} \left(\nabla(\delta_t \varepsilon_N^{k+1} + \Pi_N \nabla \cdot \tilde{e}_N^{k+1}), \nabla(\delta_t \psi_N^k + \Pi_N \nabla \cdot \tilde{e}_N^k) \right) \\ & = 2\delta t \left(\delta_t \tilde{e}_N^{k+1}, \nabla(\delta_t \psi_N^k + \Pi_N \nabla \cdot \tilde{e}_N^k) \right) + \frac{4\delta t^2}{3} \|\nabla(\delta_t \psi_N^k + \Pi_N \nabla \cdot \tilde{e}_N^k)\|^2. \end{aligned}$$

By summing up the above relations, we derive

$$\begin{aligned} & 3\|\delta_t e_N^{k+1}\|^2 + \frac{4\delta t^2}{3} \|\nabla(\delta_t \varepsilon_N^{k+1} + \Pi_N \nabla \cdot \tilde{e}_N^{k+1})\|^2 \\ & = 3\|\delta_t \tilde{e}_N^{k+1}\|^2 + 4\delta t \left(\delta_t \tilde{e}_N^{k+1}, \nabla(\delta_t \psi_N^k + \Pi_N \nabla \cdot \tilde{e}_N^k) \right) + \frac{4\delta t^2}{3} \|\nabla(\delta_t \psi_N^k + \Pi_N \nabla \cdot \tilde{e}_N^k)\|^2. \end{aligned} \quad (30)$$

We now give a bound for the last two terms in the right-hand side of (30). First, the term $4\delta t(\delta_t \tilde{e}_N^{k+1}, \nabla \delta_t \psi_N^k)$ cancels out with the same term in (29). Using relation (15), we derive

$$\begin{aligned} & 4\delta t(\delta_t \tilde{e}_N^{k+1}, \nabla \Pi_N \nabla \cdot \tilde{e}_N^k) \\ & = -4\delta t(\nabla \cdot (\tilde{e}_N^{k+1} - \tilde{e}_N^k), \Pi_N \nabla \cdot \tilde{e}_N^k) \\ & = -4\delta t(\Pi_N \nabla \cdot \tilde{e}_N^{k+1} - \Pi_N \nabla \cdot \tilde{e}_N^k, \Pi_N \nabla \cdot \tilde{e}_N^k) \\ & = 2\delta t(\|\Pi_N \nabla \cdot \tilde{e}_N^k\|^2 - \|\Pi_N \nabla \cdot \tilde{e}_N^{k+1}\|^2 + \|\Pi_N \nabla \cdot \delta_t \tilde{e}_N^{k+1}\|^2) \\ & \leq 2\delta t(\|\Pi_N \nabla \cdot \tilde{e}_N^k\|^2 - \|\Pi_N \nabla \cdot \tilde{e}_N^{k+1}\|^2 + \|\nabla \cdot \delta_t \tilde{e}_N^{k+1}\|^2). \end{aligned} \quad (31)$$

From the well-known relation

$$\|\nabla v\|^2 = \|\nabla \cdot v\|^2 + \|\nabla \times v\|^2, \quad \forall v \in H_0^1(\Omega)^2, \quad (32)$$

we deduce

$$\|\nabla \cdot \delta_t \tilde{e}_N^{k+1}\|^2 \leq \|\nabla \delta_t \tilde{e}_N^{k+1}\|^2. \quad (33)$$

Noting that $\psi_N^k = \varepsilon_N^k - \delta_t \Pi_N^1 p^{k+1}$, we can bound $\|\nabla(\delta_t \psi_N^k + \Pi_N \nabla \cdot \tilde{e}_N^k)\|^2$ by

$$\begin{aligned} & \|\nabla(\delta_t \psi_N^k + \Pi_N \nabla \cdot \tilde{e}_N^k)\|^2 \\ & = \|\nabla(\delta_t \varepsilon_N^k + \Pi_N \nabla \cdot \tilde{e}_N^k) - \nabla \delta_t \Pi_N^1 p^{k+1}\|^2 \\ & \leq \left(\|\nabla(\delta_t \varepsilon_N^k + \Pi_N \nabla \cdot \tilde{e}_N^k)\| + c\delta t^2 \right)^2 \\ & \leq c\delta t^4 + 2c\delta t^2 \|\nabla(\delta_t \varepsilon_N^k + \Pi_N \nabla \cdot \tilde{e}_N^k)\| + \|\nabla(\delta_t \varepsilon_N^k + \Pi_N \nabla \cdot \tilde{e}_N^k)\|^2 \\ & \leq c\delta t^4 + c\delta t \left(\delta t^2 + \|\nabla(\delta_t \varepsilon_N^k + \Pi_N \nabla \cdot \tilde{e}_N^k)\|^2 \right) + \|\nabla(\delta_t \varepsilon_N^k + \Pi_N \nabla \cdot \tilde{e}_N^k)\|^2 \\ & \leq c\delta t^3 + (1 + c\delta t) \|\nabla(\delta_t \varepsilon_N^k + \Pi_N \nabla \cdot \tilde{e}_N^k)\|^2. \end{aligned} \quad (34)$$

We combine the above estimations and choose c_1, c_2 in (29) to satisfy $c_1\bar{c} + c_2 = 2$, then we obtain

$$\begin{aligned} & 3\|\delta_t e_N^{k+1} - \delta_t \tilde{e}_N^{k+1}\|^2 + \|\delta_t e_N^{k+1}\|^2 + \|2\delta_t e_N^{k+1} - \delta_t e_N^k\|^2 + 2\delta t \|\Pi_N \nabla \cdot \tilde{e}_N^{k+1}\|^2 \\ & \quad + \frac{4}{3}\delta t^2 \|\nabla(\delta_t \varepsilon_N^{k+1} + \Pi_N \nabla \cdot \tilde{e}_N^{k+1})\|^2 \\ & \leq \|\delta_t e_N^k\|^2 + \|2\delta_t e_N^k - \delta_t e_N^{k-1}\|^2 + 2\delta t \|\Pi_N \nabla \cdot \tilde{e}_N^k\|^2 + c\delta t^5 \\ & \quad + \frac{4}{3}\delta t^2(1 + c\delta t) \|\nabla(\delta_t \varepsilon_N^k + \Pi_N \nabla \cdot \tilde{e}_N^k)\|^2 + c\delta t \|\delta_t R^{k+1}\|^2 + c\delta t \|\delta_t Q^{k+1}\|^2. \end{aligned} \quad (35)$$

Taking the sum of (35) for $k = 1$ to n gives

$$\begin{aligned} & \sum_{k=1}^n \|\delta_t e_N^{k+1} - \delta_t \tilde{e}_N^{k+1}\|^2 + \|\delta_t e_N^{n+1}\|^2 + \|2\delta_t e_N^{n+1} - \delta_t e_N^n\|^2 + \delta t \|\Pi_N \nabla \cdot \tilde{e}_N^{n+1}\|^2 \\ & \quad + \delta t^2 \|\nabla(\delta_t \varepsilon_N^{n+1} + \Pi_N \nabla \cdot \tilde{e}_N^{n+1})\|^2 \\ & \leq c \left(\delta t^4 + \|\delta_t e_N^1\|^2 + \|2\delta_t e_N^1 - \delta_t e_N^0\|^2 + \delta t \|\Pi_N \nabla \cdot \tilde{e}_N^1\|^2 \right. \\ & \quad \left. + \delta t^2 \|\nabla(\delta_t \varepsilon_N^1 + \Pi_N \nabla \cdot \tilde{e}_N^1)\|^2 + \delta t^3 \sum_{k=1}^n \|\nabla(\delta_t \varepsilon_N^k + \Pi_N \nabla \cdot \tilde{e}_N^k)\|^2 \right. \\ & \quad \left. + \delta t \sum_{k=1}^n \|\delta_t R^{k+1}\|^2 + \delta t \sum_{k=1}^n \|\delta_t Q^{k+1}\|^2 \right). \end{aligned} \quad (36)$$

By using the discrete Gronwall lemma to the above inequality and taking into account the initial hypotheses, we obtain the first two desired results

$$\begin{aligned} & \sum_{k=1}^n \|\delta_t e_N^{k+1} - \delta_t \tilde{e}_N^{k+1}\|^2 + \delta t^2 \|\nabla(\delta_t \varepsilon_N^{n+1} + \Pi_N \nabla \cdot \tilde{e}_N^{n+1})\|^2 + \delta t \|\Pi_N \nabla \cdot \tilde{e}_N^{n+1}\|^2 \\ & \leq c\delta t^2 \left(\delta t^2 + N^{-2m} \right). \end{aligned} \quad (37)$$

To derive the estimate on $e_N^{k+1} - \tilde{e}_N^{k+1}$, we use the first equation of (25) with $v_N = e_N^{k+1} - \tilde{e}_N^{k+1}$. Noting $\psi_N^k = \varepsilon_N^k - \delta_t \Pi_N^1 p^{k+1}$ and above estimates, then we have

$$\begin{aligned} \|e_N^{n+1} - \tilde{e}_N^{n+1}\| & \leq c\delta t \|\nabla(\varepsilon_N^{n+1} - \psi_N^n + \Pi_N \nabla \cdot \tilde{e}_N^{n+1})\| \\ & \leq c\delta t \|\nabla(\delta_t \varepsilon_N^{n+1} + \Pi_N \nabla \cdot \tilde{e}_N^{n+1})\| + \delta t \|\nabla \delta_t \Pi_N^1 p^{n+1}\| \\ & \leq c\delta t(\delta t + N^{-m}). \end{aligned} \quad (38)$$

Theorem 3.1. *Under the initial hypotheses (18), the solution of the projection scheme (13)-(14) satisfies:*

$$\|u - u_N\|_{l^2(L^2(\Omega)^2)} + \|u - \tilde{u}_N\|_{l^2(L^2(\Omega)^2)} \leq c(\delta t^2 + N^{-m}). \quad (39)$$

Proof. From (24)-(25), we derive

$$\begin{aligned} & \left(\frac{3e_N^{k+1} - 4e_N^k + e_N^{k-1}}{2\delta t}, v_N \right) + (\nabla \tilde{e}_N^{k+1}, \nabla v_N) + \left(\nabla(\varepsilon_N^{k+1} + \Pi_N \nabla \cdot \tilde{e}_N^{k+1}), v_N \right) \\ & = (R^{k+1}, v_N) + (Q^{k+1}, \nabla \cdot v_N), \quad \forall v_N \in X_N. \end{aligned} \quad (40)$$

Taking $v_N = 4\delta t S_N e_N^{k+1}$ in (40), we get

$$\begin{aligned} & 2(3e_N^{k+1} - 4e_N^k + e_N^{k-1}, S_N e_N^{k+1}) + 4\delta t \left(\nabla \tilde{e}_N^{k+1}, \nabla(S_N e_N^{k+1}) \right) + 4\delta t \left(\nabla(\varepsilon_N^{k+1} + \Pi_N \nabla \cdot \tilde{e}_N^{k+1}), S_N e_N^{k+1} \right) \\ & = 4\delta t(R^{k+1}, S_N e_N^{k+1}) + 4\delta t(Q^{k+1}, \nabla \cdot S_N e_N^{k+1}). \end{aligned}$$

From the definition of S_N , we have,

$$4\delta t \left(\nabla(\varepsilon_N^{k+1} + \Pi_N \nabla \cdot \tilde{e}_N^{k+1}), S_N e_N^{k+1} \right) = 0.$$

By the property (4), we derive the following identity which is similar to (16):

$$2(3e_N^{k+1} - 4e_N^k + e_N^{k-1}, S_N e_N^{k+1}) = \|e_N^{k+1}\|_{\star}^2 + \|2e_N^{k+1} - e_N^k\|_{\star}^2 + \|\delta_{tt} e_N^{k+1}\|_{\star}^2 - \|e_N^k\|_{\star}^2 - \|2e_N^k - e_N^{k-1}\|_{\star}^2.$$

Hence

$$\begin{aligned} & \|e_N^{k+1}\|_*^2 + \|2e_N^{k+1} - e_N^k\|_*^2 + \|\delta_{tt}e_N^{k+1}\|_*^2 + 4\delta t(\nabla\tilde{e}_N^{k+1}, \nabla(S_N e_N^{k+1})) \\ & \leq \|e_N^k\|_*^2 + \|2e_N^k - e_N^{k-1}\|_*^2 + 4\delta t(S_N e_N^{k+1}, R^{k+1}) + 4\delta t(\nabla \cdot S_N e_N^{k+1}, Q^{k+1}). \end{aligned}$$

Using the identity $e_N^{k+1} = P_{H_N}\tilde{e}_N^{k+1}$ and (8) with $\alpha = \frac{1}{4}$, we derive

$$\begin{aligned} & \|e_N^{k+1}\|_*^2 + \|2e_N^{k+1} - e_N^k\|_*^2 + \|\delta_{tt}e_N^{k+1}\|_*^2 + 3\delta t\|e_N^{k+1}\|_*^2 \\ & \leq \|e_N^k\|_*^2 + \|2e_N^k - e_N^{k-1}\|_*^2 + c\delta t\|e_N^{k+1} - \tilde{e}_N^{k+1}\|_*^2 \\ & \quad + 4\delta t(S_N e_N^{k+1}, R^{k+1}) + 4\delta t(\nabla \cdot S_N e_N^{k+1}, Q^{k+1}). \end{aligned} \tag{41}$$

The last two terms can be bounded by using (5) :

$$4\delta t(S_N e_N^{k+1}, R^{k+1}) \leq 4\delta t\|S_N e_N^{k+1}\| \|R^{k+1}\| \leq \frac{1}{2}\delta t\|e_N^{k+1}\|_*^2 + c\delta t\|R^{k+1}\|^2. \tag{42}$$

$$4\delta t(\nabla \cdot S_N e_N^{k+1}, Q^{k+1}) \leq 4\delta t\|S_N e_N^{k+1}\|_1 \|Q^{k+1}\| \leq \frac{1}{2}\delta t\|e_N^{k+1}\|_*^2 + c\delta t\|Q^{k+1}\|^2. \tag{43}$$

Combining (41)-(43) and taking the sum of (41) for $k = 1$ to n , we have

$$\begin{aligned} & \|e_N^{n+1}\|_*^2 + \|2e_N^{n+1} - e_N^n\|_*^2 + \sum_{k=1}^n \|\delta_{tt}e_N^{k+1}\|_*^2 + \delta t \sum_{k=1}^n \|e_N^{k+1}\|_*^2 \\ & \leq \|e_N^1\|_*^2 + \|2e_N^1 - e_N^0\|_*^2 + c\delta t \sum_{k=1}^n \|e_N^{k+1} - \tilde{e}_N^{k+1}\|_*^2 + \delta t \sum_{k=1}^n \|e_N^{k+1}\|_*^2 + c(\delta t^4 + N^{-2m}). \end{aligned}$$

Applying the discrete Gronwall lemma, estimates (38), and the initial hypotheses (18), we get

$$\|e_N\|_{l^2(L^2(\Omega)^2)} \leq c(\delta t^2 + N^{-m}).$$

Furthermore, thanks to the relations

$$\|\tilde{e}_N^{k+1}\| \leq \|e_N^{k+1} - \tilde{e}_N^{k+1}\| + \|e_N^{k+1}\|,$$

and

$$u_N^k - u^k = e_N^k + \Pi_N^0 u^k - u^k, \quad \tilde{u}_N^k - u^k = \tilde{e}_N^k + \Pi_N^0 u^k - u^k,$$

we arrive at the desired result.

Lemma 3.2. *Under the hypotheses (18), we have*

$$\|D_t \tilde{e}_N\|_{l^2(L^2(\Omega)^2)} \leq c\delta t(\delta t^{3/2} + N^{-m}). \tag{44}$$

Proof. we obtain the following equation from (26)-(27):

$$\begin{aligned} & \left(\frac{3\delta t\tilde{e}_N^{k+1} - 4\delta t\tilde{e}_N^k + \delta t\tilde{e}_N^{k-1}}{2\delta t}, v_N \right) + (\nabla\delta_t\tilde{e}_N^{k+1}, \nabla v_N) + (\nabla\delta_t\gamma_N^{k+1}, v_N) \\ & = (\delta_t R^{k+1}, v_N) + (\delta_t Q^{k+1}, \nabla \cdot v_N), \quad \forall v_N \in X_N, \end{aligned} \tag{45}$$

where $\delta_t\gamma_N^{k+1}$ represents all the other terms which belong to M_N . Taking $v_N = 4\delta tS_N\delta_t\tilde{e}_N^{k+1} \in V_N$ in (45) and repeating the same arguments as in the theorem 3.1 and using the inequality (7), we obtain

$$\begin{aligned} & \|\delta_t\tilde{e}_N^{k+1}\|_*^2 + \|2\delta_t\tilde{e}_N^{k+1} - \delta_t\tilde{e}_N^k\|_*^2 + \|\delta_{ttt}\tilde{e}_N^{k+1}\|_*^2 + \delta t\|\delta_t\tilde{e}_N^{k+1}\|_*^2 \\ & \leq \|\delta_t\tilde{e}_N^k\|_*^2 + \|2\delta_t\tilde{e}_N^k - \delta_t\tilde{e}_N^{k-1}\|_*^2 + c\delta t\|\delta_t\tilde{e}_N^{k+1}\|_*^2 \\ & \quad + c\delta t\|\delta_t\tilde{e}_N^{k+1} - \delta_t e_N^{k+1}\|_*^2 + c\delta t\|\delta_t R^{k+1}\|^2 + c\delta t\|\delta_t Q^{k+1}\|^2. \end{aligned} \tag{46}$$

Summing the above relations for $k = 1$ to n , we have

$$\begin{aligned} & \|\delta_t\tilde{e}_N^{n+1}\|_*^2 + \|2\delta_t\tilde{e}_N^{n+1} - \delta_t\tilde{e}_N^n\|_*^2 + \delta t \sum_{k=1}^n \|\delta_t\tilde{e}_N^{k+1}\|_*^2 \\ & \leq \|\delta_t\tilde{e}_N^1\|_*^2 + \|2\delta_t\tilde{e}_N^1 - \delta_t\tilde{e}_N^0\|_*^2 + c\delta t \sum_{k=1}^n \|\delta_t\tilde{e}_N^{k+1}\|_*^2 \\ & \quad + c\delta t \sum_{k=1}^n \|\delta_t\tilde{e}_N^{k+1} - \delta_t e_N^{k+1}\|_*^2 + c\delta t \sum_{k=1}^n \|\delta_t R^{k+1}\|^2 + c\delta t \sum_{k=1}^n \|\delta_t Q^{k+1}\|^2. \end{aligned} \tag{47}$$

By the discrete Gronwall lemma and the initial hypotheses (18), we have

$$\|\delta_t \tilde{e}_N\|_{l^2(L^2(\Omega)^2)} \leq c\delta t(\delta t^{3/2} + N^{-m}).$$

Finally from the relation $2D_t \tilde{e}_N^{k+1} = 3\delta_t \tilde{e}_N^{k+1} - \delta_t \tilde{e}_N^k$, we derive (44).

Theorem 3.2. *Under the hypotheses (18), the solution of the projection scheme (13)-(14) satisfies:*

$$\|u - \tilde{u}_N\|_{l^2(H^1(\Omega)^2)} + \beta_N \|p - p_N\|_{l^2(L^2(\Omega))} \leq c(\delta t^{3/2} + N^{-m}). \quad (48)$$

Proof. We use the same argument as in [14]. The error equations corresponding to (40) and (25) can be written as a discrete nonhomogeneous Stokes system for the couple $(\tilde{e}_N^{k+1}, \varepsilon_N^{k+1} + \Pi_N \nabla \cdot \tilde{e}_N^{k+1}) \in X_N \times M_N$:

$$\begin{cases} (\nabla \tilde{e}_N^{k+1}, \nabla v_N) - ((\varepsilon_N^{k+1} + \Pi_N \nabla \cdot \tilde{e}_N^{k+1}), \nabla \cdot v_N) = (h^{k+1}, v_N), & \forall v_N \in X_N, \\ (\nabla \cdot \tilde{e}_N^{k+1}, q_N) = (g^{k+1}, q_N), & \forall q_N \in M_N, \end{cases} \quad (49)$$

where

$$\begin{aligned} h^{k+1} &= R^{k+1} - \frac{3e_N^{k+1} - 4e_N^k + e_N^{k-1}}{2\delta t} - \nabla Q^{k+1}, \\ g^{k+1} &= \frac{2\delta t}{3} \nabla \cdot \nabla (\varepsilon^{k+1} - \psi_N^k + \Pi_N \nabla \cdot \tilde{e}_N^{k+1}). \end{aligned}$$

Since $e_N^k = P_{H_N} \tilde{e}_N^k$, we obtain

$$\left\| \frac{3e_N^{k+1} - 4e_N^k + e_N^{k-1}}{2\delta t} \right\| = \frac{1}{\delta t} \|D_t e_N^{k+1}\| \leq \frac{1}{\delta t} \|D_t \tilde{e}_N^{k+1}\|.$$

Hence, we have

$$\begin{aligned} \|h^{k+1}\|_{-1} &\leq \|R^{k+1}\|_{-1} + \left\| \frac{3e_N^{k+1} - 4e_N^k + e_N^{k-1}}{2\delta t} \right\|_{-1} + \|\nabla Q^{k+1}\|_{-1} \\ &\leq \|R^{k+1}\| + \frac{1}{\delta t} \|D_t \tilde{e}_N^{k+1}\| + \|\nabla Q^{k+1}\|_{-1} \\ &\leq c(\delta t^{3/2} + N^{-m}). \end{aligned} \quad (50)$$

From the second equation of (49), we have

$$(g^{k+1}, q_N) = (\nabla \cdot \tilde{e}_N^{k+1}, q_N) = (\Pi_N \nabla \cdot \tilde{e}_N^{k+1}, q_N), \quad \forall q_N \in M_N,$$

then

$$\|g^{k+1}\| \leq \|\Pi_N \nabla \cdot \tilde{e}_N^{k+1}\| \leq c\delta t^{1/2}(\delta t + N^{-m}). \quad (51)$$

Applying the standard stability result ([4]) to the non-homogeneous Stokes systems (49), we obtain

$$\|\tilde{e}_N^{k+1}\|_1 + \beta_N \|\varepsilon_N^{k+1} + \Pi_N \nabla \cdot \tilde{e}_N^{k+1}\| \leq c(\|h^{k+1}\|_{-1} + \|g^{k+1}\|).$$

Now we use the triangle inequality to get

$$\begin{aligned} \|\varepsilon_N^{k+1}\| &= \|\varepsilon_N^{k+1} + \Pi_N \nabla \cdot \tilde{e}_N^{k+1} - \Pi_N \nabla \cdot \tilde{e}_N^{k+1}\| \\ &\leq \|\varepsilon_N^{k+1} + \Pi_N \nabla \cdot \tilde{e}_N^{k+1}\| + \|\Pi_N \nabla \cdot \tilde{e}_N^{k+1}\|. \end{aligned}$$

Therefore

$$\|\tilde{e}_N^{k+1}\|_1 + \beta_N \|\varepsilon_N^{k+1}\| \leq \beta_N \|\Pi_N \nabla \cdot \tilde{e}_N^{k+1}\| + c(\|h^{k+1}\|_{-1} + \|g^{k+1}\|) \leq c(\delta t^{3/2} + N^{-m}).$$

Thanks to above relations, we derive

$$\|\tilde{e}_N\|_{l^2(H^1(\Omega)^2)} + \beta_N \|\varepsilon_N\|_{l^2(L^2(\Omega))} \leq c(\delta t^{3/2} + N^{-m}).$$

Finally, using the relations

$$\tilde{u}_N^k - u^k = \tilde{\epsilon}_N^k + \Pi_N^0 u^k - u^k, \quad p_N^k - p^k = \epsilon^k + \Pi_N^1 p^k - p^k,$$

the desired result is obtained.

4. Numerical Results

In order to test the accuracy of the projection schemes, a Stokes problem with an analytical solution is solved. Numerical experiences are carried out using $P_N \times P_N$ Legendre spectral methods for the spatial approximation, although theoretical analysis has been done in the frame of $P_N \times P_{N-2}$ version. This is for the following reasons: First, numerical tests using $P_N \times P_{N-2}$ spectral projection schemes (mono-domain case) have been carried out by Guermond and Shen in their recent paper [14], where desired convergence rate has been obtained; Second, in view of computational efficiency, it is highly hopeful to use $P_N \times P_N$ version that allows to produce a true discrete Laplacian system. Such a system is much easier to solve than a pseudo-Laplacian stemming from a $P_N \times P_{N-2}$ spectral method (see e.g. [3, 1]); Third, analysis shows that $P_N \times P_N$ projection scheme is a spurious mode-free method, contrast to the usual point of view that $P_N \times P_N$ spectral methods suffer still from the space incompatibility, which is generally present when the velocity and pressure is solved in coupled form. In fact it is easy to check that all classical pressure spurious modes, such as $L'_N(x)L'_N(y), L_0(x)L_N(y), \dots$ (see e.g. [4], proposition 5.2), are excluded if we compute the pressure by problem (14). Recently reported instability [2] in the use of the $P_N \times P_N$ version in the frame of projection methods is probably caused by the inconsistent pressure boundary conditions at the corners, as already indicated by some authors (see e.g. [30]). As we will see in the following numerical tests, this eventual instability can be efficiently overcome by using a simple filtering procedure, and desired convergence rate is then recovered.

Precisely, the following full discretization is used in our numerical experiences: for $k = 1, 2, \dots$, find $\tilde{u}_N^k \in X_N, u_N^k \in Y_N$ and $p_N^k \in M'_N$ such that

$$\begin{aligned} & \left(\frac{3\tilde{u}_N^{k+1} - 4u_N^k + u_N^{k-1}}{2\delta t}, v_N \right) + \nu(\nabla \tilde{u}_N^{k+1}, \nabla v_N) - (p_N^k, \nabla \cdot v_N) \\ & = (f^{k+1}, v_N), \quad \forall v_N \in X_N, \end{aligned}$$

and

$$\begin{cases} \left(\frac{3u_N^{k+1} - 3\tilde{u}_N^{k+1}}{2\delta t}, v_N \right) + \left(\nabla(p_N^{k+1} - p_N^k + \nu \Pi_N \nabla \cdot \tilde{u}_N^{k+1}), v_N \right) = 0, & \forall v_N \in Y_N, \\ (u_N^{k+1}, \nabla q_N) = 0, & \forall q_N \in M'_N. \end{cases}$$

where $M'_N = M \cap P_N(\Omega)$, different with the definition of M_N used in (13)-(14). At each time step, once $p_N^{k+1} - p_N^k + \nu \Pi_N \nabla \cdot \tilde{u}_N^{k+1}$ is obtained, we project it into the space $M_N = M \cap P_{N-2}(\Omega)$ (see [22] for a related description). This formulation is formally close to (13)-(14), but they are not equivalent. The former allows use of a unique mesh, which can greatly reduce the computational complexity. More importantly, we will show by numerical tests that the new formulation possesses the desired accuracy same as (13)-(14), as predicted by our theoretical analysis.

The exact solution (u, p) of the Stokes equations is set to be:

$$\begin{cases} u_1(x, y, t) = \sin(t) \sin(2\pi x) \cos(2\pi y), \\ u_2(x, y, t) = -\sin(t) \cos(2\pi x) \sin(2\pi y), \\ p(x, y, t) = \sin^2(t) \cos(\pi x) \sin(\pi y), \end{cases} \tag{52}$$

the source term is given by $f = u_t - \nu \Delta u + \nabla p$:

$$\begin{cases} f_1 = [\cos(t) + 8\nu\pi^2 \sin(t)] \sin(2\pi x) \cos(2\pi y) - \pi \sin^2(t) \sin(\pi x) \sin(\pi y), \\ f_2 = [-\cos(t) - 8\nu\pi^2 \sin(t)] \cos(2\pi x) \sin(2\pi y) + \pi \sin^2(t) \cos(\pi x) \cos(\pi y), \end{cases} \tag{53}$$

with zero initial condition and time-dependent boundary conditions for the velocity according to the exact solution. We take $\nu = 0.1$ except stated otherwise.

4.1 Mono-domain spectral approximation

Now we solve the above problem on the domain $\Omega = (0, 1) \times (0, 1)$. In the first test, we take N large enough such that the spatial discretization errors are negligible as compared with the time discretization errors. Then a small enough time step is fixed in order to study the spatial errors. All errors are calculated up to $T = 1$.

In Figure 1, we plot pressure error fields at $T = 1$ for a typical time step $\delta t = 0.01$ with $N = 38$. We see that for the standard form of the projection schemes, a numerical boundary layer appears on the two boundaries where the exact pressure is such that $\frac{\partial p}{\partial \mathbf{n}} \neq 0$ (*i.e.* the boundaries $y = 0$ or $y = 1$). For the rotational form, there is no numerical boundary layer, but we observe larger spikes at the four corners of the domain. In order to know whether the larger spikes at the corners are caused by the use of $P_N \times P_N$ methods, we filter the pressure solution by projecting it into P_{N-2} space at each time step. The filtered errors are shown in the two down figures in Figure 1. It is seen that the filtering has no effect on the standard form, but efficiently smoothes the spikes on the error plot given by the rotational form. These observations indicate that the divergence correction in the rotational projection methods successfully cured the numerical boundary layer problem, and the filtered $P_N \times P_N$ spectral methods recovered the accuracy that $P_N \times P_{N-2}$ methods possess (see [14]).

It is worth noting that although more accurate than the standard projection methods, the filtered $P_N \times P_N$, like $P_N \times P_{N-2}$ rotational projection methods suffer still the corner problem. Larger errors on the corners do not seem due to the classical spurious modes since any eventual such modes would already have been removed by the filtering. It is mostly related to the fact that the use of a Neumann condition overdetermines the problem at the corner points [30]. This point will be further confirmed by the following tests using spectral element methods.

In Figure 2, we compare the errors on the velocity measured in various norms as functions of the time step δt . Comparison on the pressure errors is given in Figure 3. As expected, for the velocity in the norms $l^2(L^2(\Omega)^2)$ and $l^2(H^1(\Omega)^2)$, both the rotational projection schemes and the standard one attain 2-order convergence. The filtering procedure does not allow to increase the convergence rate, but allows to improve the accuracy, as shown in the right graph of Figure 2. For the pressure, as shown in Figure 3, the errors on the norm $l^2(L^2(\Omega))$ are not fully 3/2-order for the non-filtering $P_N \times P_N$ version because of the larger errors at the corners of the domain. Precisely, $l^2(L^2(\Omega))$ norm errors are 3/2-order only for moderate time steps while it doesn't remain true for small time steps (Figure 3, left). However for a reason not yet clear, the errors in the norms $l^2(H^1(\Omega))$ are only 1-order for the non-filtering $P_N \times P_N$ version while 3/2-order is obtained for the filtered $P_N \times P_N$ version, specially for the rotational form. Furthermore, the right graph of Figure 3 shows that, even higher order convergence rate than 3/2 is obtained for the pressure errors in the norm $l^2(L^2(\Omega))$ by using filtered $P_N \times P_N$ version. In summary, the rotational form and filtered version are more accurate than the standard form and simple version for both velocity and pressure. All the following tests are carried out with the filtered $P_N \times P_N$ version.

In Figure 4, spatial accuracy of the rotational projection spectral methods are investigated by plotting the errors in norm $l^2(L^2(\Omega))$ as functions of the polynomial degree N . From the left graph of the figure, the spectral convergence is obvious for both the velocity and pressure solutions. Influence of the viscosity ν on the accuracy is also studied. In the right graph of the figure, the errors for several values of ν are plotted. It is seen that the velocity errors are almost independent of ν , while the pressure errors decrease quickly when ν decreases. This observation offers additional support to the suggestion that the pressure error spikes at the corners are related to inconsistent pressure conditions at the corners.

4.2 Spectral element approximation

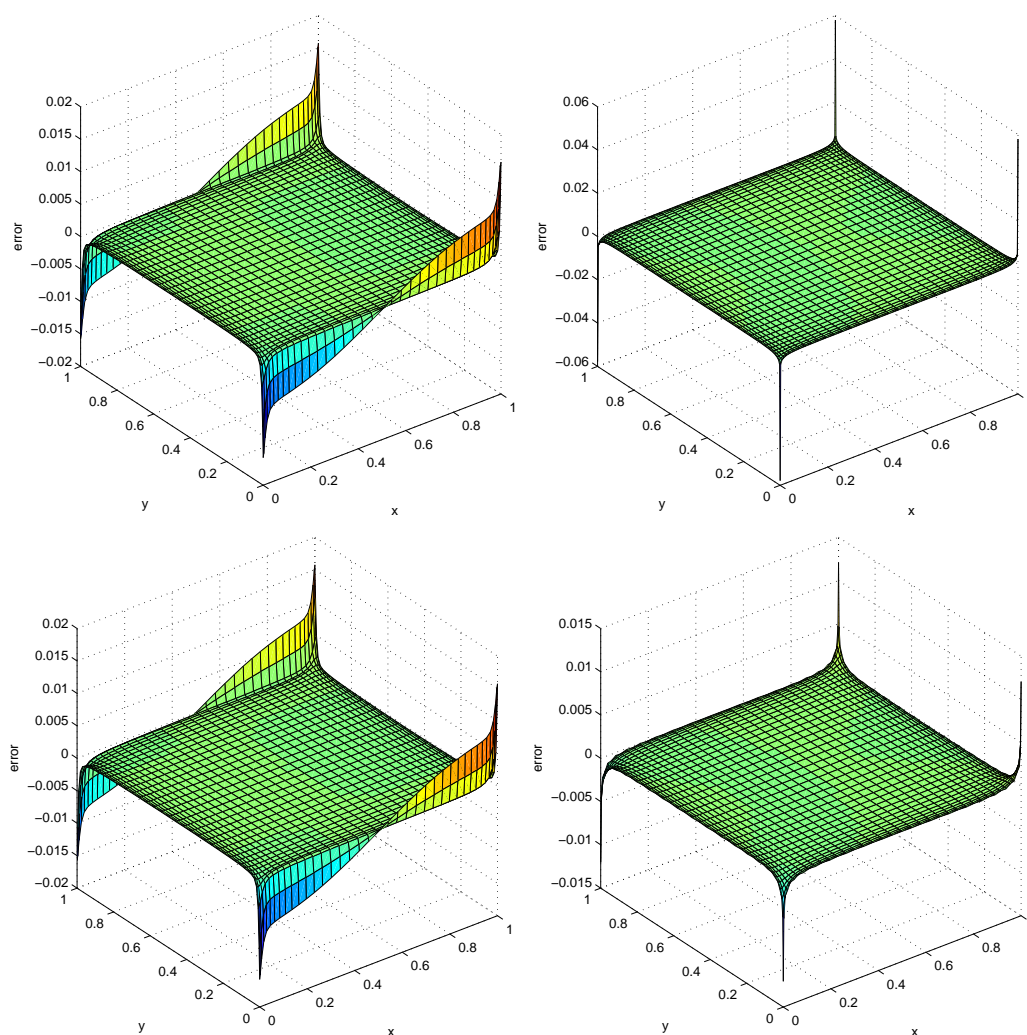


Figure 1: Pressure error fields at $T = 1$ with $\delta t = 0.01$ and $N = 38$ for the projection spectral methods. Up: $P_N \times P_N$ version; down: filtered $P_N \times P_N$ version. Left: standard form; right: rotational form.

The above numerical experiences are repeated in the case of spectral element methods (SEM) and we successively study:

- Influence of the domain decomposition;
- Convergence behavior in the case of smooth domain.

Implementation of the projection schemes in the $P_N \times P_N$ SEM depends essentially on the formulation of the pressure system. The easiest way to discretize the Laplacian system for the pressure is to define the discrete pressure in the $(N + 1)^2$ Gauss-Lobatto collocation points in each macro-element. In such a way, there are pressure nodes located on the elemental interfaces, hence continuity of the pressure on the interfaces can be naturally imposed.

First we take the domain $\Omega = (0, 1) \times (0, 1)$ which is divided into 4 equal square elements. In order to check the temporal accuracy, the computation is run up to $T = 1$ using polynomial degree N large enough such that the spatial errors are negligible as compared with the temporal errors.

In Figure 5, we draw the pressure error fields at $T = 1$ using the projection SEM with

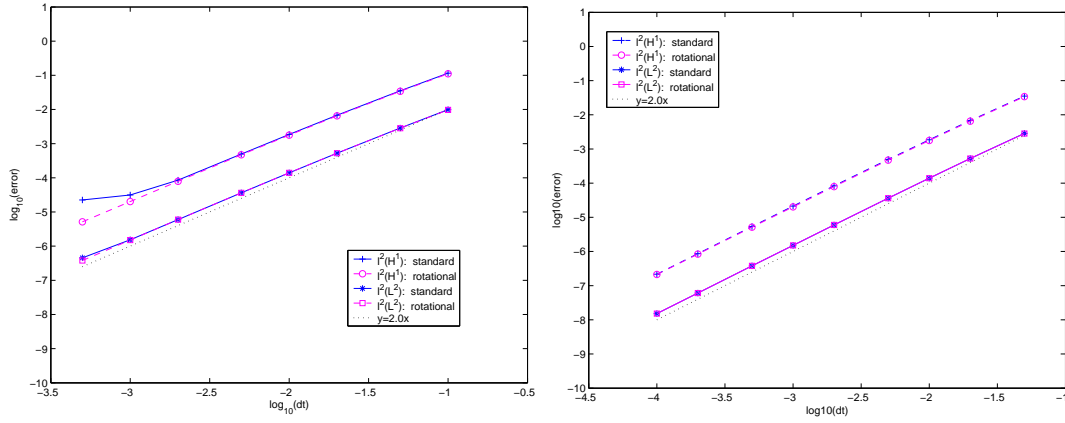


Figure 2: Errors on the velocity as a function of the time step for $N = 38$. Left: $P_N \times P_N$ version; right: filtered $P_N \times P_N$ version.

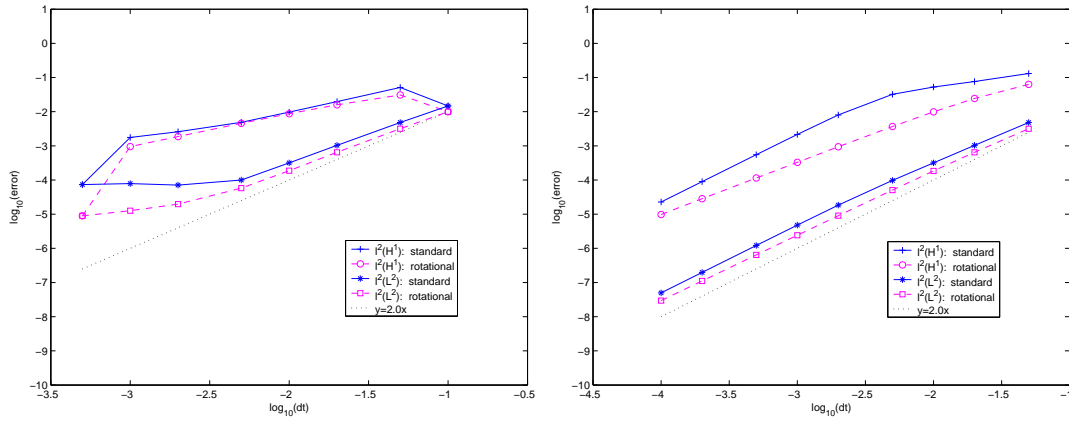


Figure 3: Errors on the pressure as a function of the time step for $N = 38$. Left: $P_N \times P_N$ version; right: filtered $P_N \times P_N$ version.

$\delta t = 0.01, N = 24$. The results are similar to the case of mono-domain: numerical boundary layer by the standard form, large spikes at the corners by the rotational form. However it is remarkable that the large spikes are only present at the four physical corners. The situation is the same for the non-filtered $P_N \times P_N$ version (results non shown). This supports our previous statement that larger pressure errors at the corners are not due to the $P_N \times P_N$ methods, but to the incompatibility of the pressure boundary conditions. In Figure 6, we plot the errors on the velocity and pressure measured in various norms as functions of the time step δt . The results are also similar to the case of mono-domain.

To clarify the role of the singularity of the boundary, we carry out a test in the circular domain $\Omega = \{(x, y) : \frac{1}{4} < x^2 + y^2 < 1\}$, which is divided into 12 equal elements. Figure 7 shows the pressure error fields computed in this smooth domain at $T = 1$ with $\delta t = 0.01, N = 16$. A numerical boundary layer exists still on the entire boundary for the pressure calculated by means of the standard form, but the errors are small everywhere for the rotational form. The results are similar to the non-filtered $P_N \times P_N$ SEM (non shown). This test confirms that the pressure oscillation at the corners is related to the singularity of the domain, not to the $P_N \times P_N$

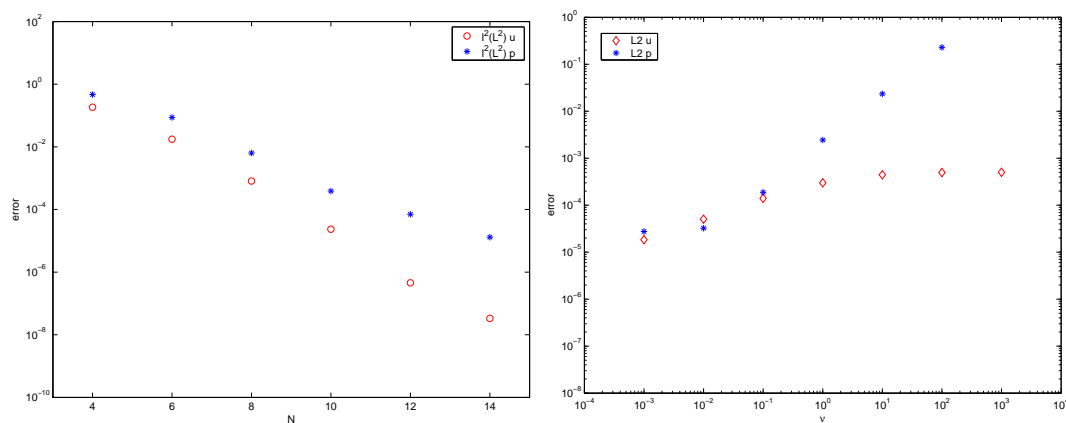


Figure 4: Left: Errors varying with the polynomial degree N (y-axis is log scale); Right: Errors varying with ν (log scale).

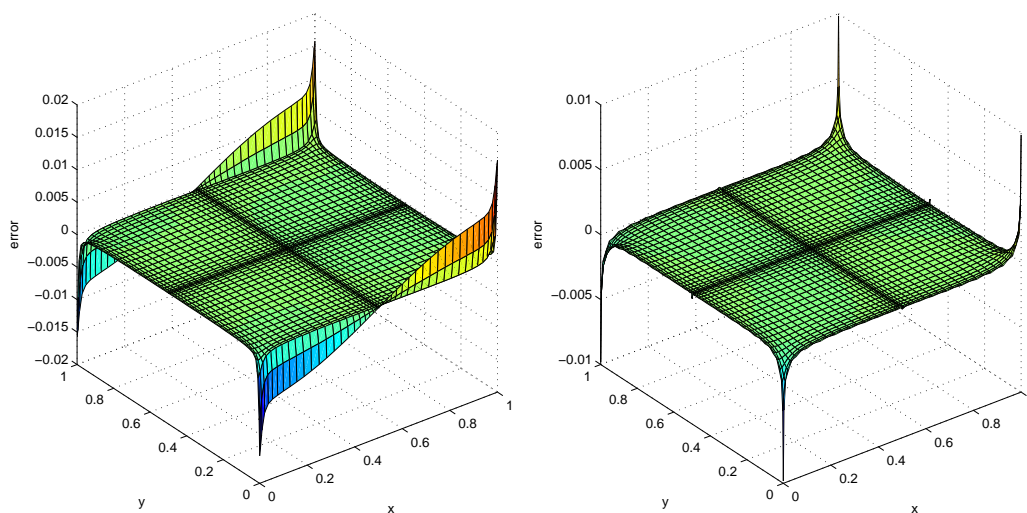


Figure 5: Pressure error fields at $T = 1$ by the projection SEM with $\delta t = 0.01$, $N = 24$. Left: standard form; right: rotational form.

method.

From the left graph of Figure 8, we observe that for the circular domain, the pressure errors measured in norm $l^2(L^2(\Omega))$ and $l^2(H^1(\Omega))$ are $3/2$ -order. The pressure errors measured in norm $L^2(\Omega)$ at time $T = 1$ are given in the right graph of Figure 8. We see that the convergence rates are now fully second order. This conforms to the results obtained in [14] and [30].

5. Concluding Remarks

There exists much works concerning numerical and theoretical investigations on the convergence rates of projection methods. We have presented in this paper a detail analysis of the rotational pressure-correction methods in the frame of the spectral spatial approximations for the unsteady Stokes equations. Error estimations for the fully discrete scheme show that

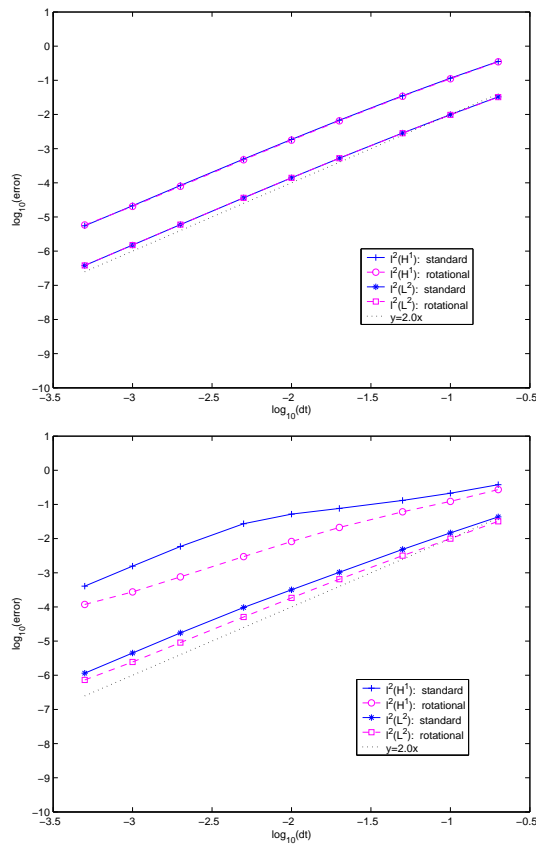


Figure 6: Velocity (left) and pressure (right) errors obtained by the projection SEM with $N = 24$ in each element.

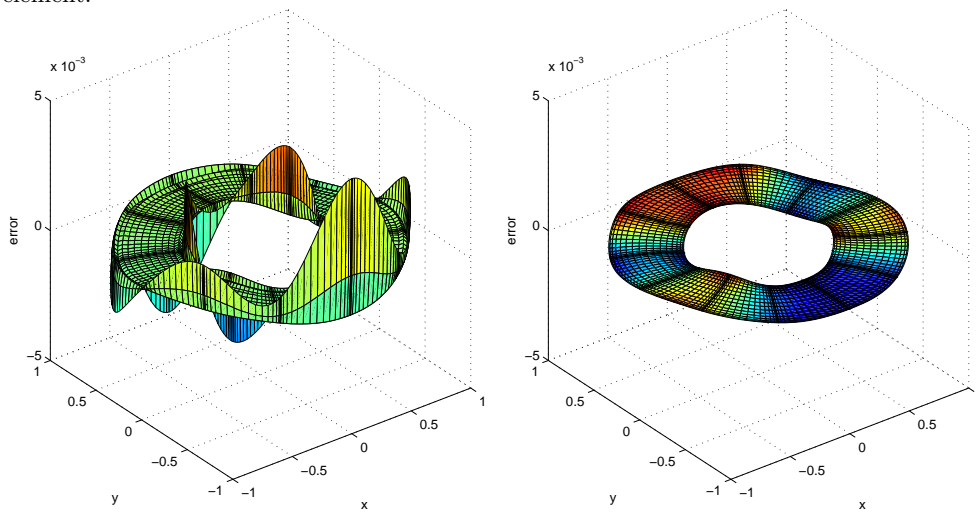


Figure 7: Pressure error fields at $T = 1$ by the projection SEM with $\delta = 0.01$ and $N = 16$ in each element. Left: standard form; right: rotational form.

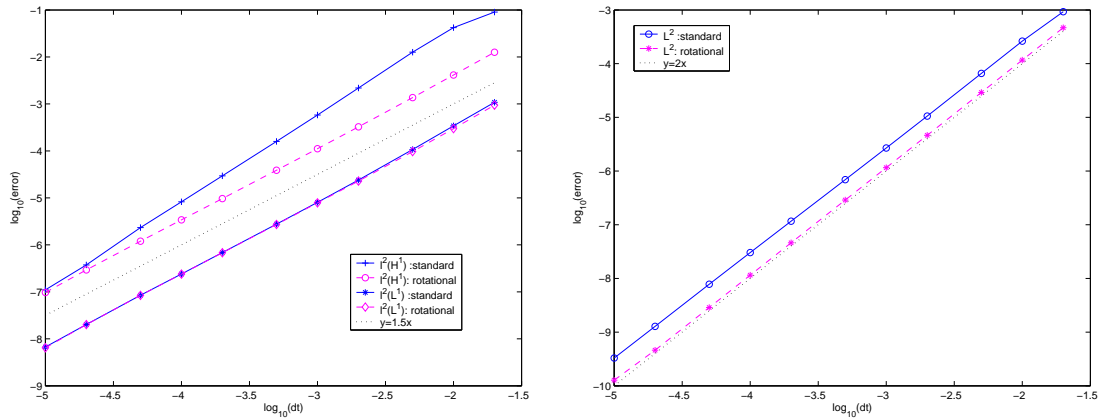


Figure 8: Convergence rates of the pressure with $N = 16$. Left: l^2 -norm; Right: L^2 -norm at time $T = 1$.

the convergence rate for the velocity in the $l^2(L^2(\Omega))$ -norm is order $O(\delta t^2 + N^{-m})$, while the convergence rate for the pressure is order $O(\delta t^{\frac{3}{2}} + N^{-m})$, with here m the regularity of the exact pressure solution.

The error estimates have been obtained by assuming that the discrete velocity and pressure space pair satisfies the LBB condition (1), precisely by using the $P_N \times P_{N-2}$ approximation. The role of the LBB conditions in the frame of the projection-type schemes has been discussed by several authors. We refer to [2, 13] for recent detail discussions in this sense.

However we would like to mention here that the compatibility assumption used in our proof for the convergence rate seems to be a technical need.

From the point of view of implementation, the LBB condition (1) between the velocity and pressure approximation space is not mandatory for the projection methods to work. Indeed, a principal interest in using the projection-type method is that we are free from the compatibility restriction on the choice of the discrete velocity and pressure space. Otherwise, the fractional step methods, which were introduced and analyzed in [21, 9, 11, 18, 31], could be the preference.

From the theoretical point of view, it is well-known that the LBB condition (1) is a necessary and sufficient condition to obtain the optimal convergence rate when the velocity and pressure are formulated in a coupled form. This is because that the well-known spurious modes (see e.g. [4], p126) may pollute the pressure if the LBB condition (1) is violated. However, when solving the velocity and pressure in two decoupled steps by the rotational projection schemes, there is no evidence showing that the LBB condition (1) is a necessary condition to guarantee the uniqueness of the pressure solution. Although numerical pressure oscillations using $P_N \times P_N$ spectral projection methods (in standard forms) with very small time steps were recently reported [2], the cause of these oscillations is not yet clear. It seems to us that the most possible reason for these oscillations is the inconsistent pressure boundary conditions, especially when the domain includes corners. In fact it is readily to see, as mentioned at the beginning of the numerical experiences, that the spurious modes presented in a coupled $P_N \times P_N$ scheme are excluded from the pressure in the projection step (14) even if the space M_N is taken to be P_N . Furthermore, our numerical experiences have shown that $P_N \times P_N$ version works well, and no numerical oscillations occur in the case where the computational domain is smooth.

Acknowledgments. We would like to thank J. Shen for his suggestion and many helpful discussions.

References

- [1] M. Azaiez et al., A unique grid spectral solver of the nD Cartesian unsteady Stokes system, Illustrative numerical results, *Finite Elem. Anal. Des.*, **16**:3-4 (1994), 247-260.
- [2] F. Auteri, J.L. Guermond, and N. Parolini, Role of the LBB condition in weak spectral projection methods, *J. Comput. Phys.*, **420** (2001), 405-420.
- [3] O. Botella, On the solution of the Navier-Stokes equations using Chebyshev projection schema with third order accuracy in time, *Computers & Fluids*, **26**:2 (1997), 107-116.
- [4] C. Bernardi, Y. Maday, Approximations spectrales de problèmes aux limites elliptiques, Springer-Verlag, Paris, 1992.
- [5] F. Brezzi, On the existence, uniqueness and approximation of saddle-point problems arising from Lagrangian multipliers, *RAIRO*, **8** (1974), 129-151.
- [6] C. Canuto, M.Y. Hussaini, A. Quarteroni, T.A. Zang, Spectral Methods in Fluid Dynamics, Springer Verlag, New York, 1988.
- [7] A.J. Chorin, Numerical solution of the Navier-Stokes equations, *Math. Comp.*, **22** (1968), 464-499.
- [8] A.J. Chorin, On the convergence of discrete approximations to the Navier-Stokes equations, *Math. Comp.*, **23** (1969), 341-353.
- [9] W. Couzy, M.O. Deville, A fast Schur complement method for the spectral element discretization of the incompressible Navier-Stokes equations, *J. Comput. Phys.*, **116** (1995), 135-142.
- [10] W. E, J.G. Liu, Projection method I: Convergence and numerical boundary layers, *SIAM J. Numer. Anal.*, **32** (1995), 1017-1057.
- [11] P. Fischer, An overlapping Schwarz method for spectral element solution of the incompressible Navier-Stokes equations, *J. Comput. Phys.*, **133** (1997), 84-101.
- [12] J.L. Guermond, L. Quartapelle, On the approximation of the unsteady Navier-Stokes equations by finite element projection methods, *Numer. Math.*, **80** (1998), 207-238.
- [13] J.L. Guermond, L. Quartapelle, On stability and convergence of projection methods based on pressure Poisson equations, *Inter. J. Numer. Methods Fluids*, **26**:9 (1998), 1039-1053.
- [14] J.L. Guermond, J. Shen, On the error estimates for the rotational pressure-correction projection methods, to appear in *Math. Comp.*.
- [15] J.L. Guermond, Un résultat de convergence d'ordre deux en temps pour l'approximation des équations de Navier-Stokes par une technique de projection, *Modél. Math. Anal. Numér.*, **33**:1 (1999), 169-189.
- [16] P.M. Gresho, R.L. Sani, On pressure boundary conditions for the incompressible Navier-Stokes equations, *Int. J. Numer. Meth. Fluids*, **7** (1987), 1111-1145.
- [17] G.E. Karniadakis, M. Israeli, S.A. Orszag, High-order splitting schemes for the incompressible Navier-Stokes equations, *J. Comp. Phys.*, **97** (1991), 414-443.
- [18] Y.M. Lin, C.J. Xu, A fractional step method for the unsteady viscous/inviscid coupled equation, to appear in Proceeding of Third International Workshop on Scientific Computing and Applications, City University of Hong Kong, Jan., 2003.
- [19] Y. Maday, D. Meiron, A.T. Patera, E.M. Ronquist, Analysis of iterative methods for the steady and unsteady Stokes problem: Application to spectral element discretization, *SIAM J. Sci. Comput.* **14**:2 (1993), 310-337.
- [20] Y. Maday, A.T. Patera, Spectral element methods for the incompressible Navier-Stokes equations, State-of-the-art surveys in computational mechanics, A.K.Noor(ed.), ASME, New York, (1988), 71-143.
- [21] J.B. Perot, An analysis of the fractional step method, *J. Comput. Phys.*, **108** (1993), 51-58.
- [22] R. Pasquetti, C.J. Xu, Note: Comments on Filter-Based Stabilization of Spectral Element Methods, *J. Comput. Phys.*, **182** (2002), 646-650.
- [23] A. Quarteroni, A. Valli, Numerical Approximation of Partial Differential Equations, Springer Verlag, New York, 1998.

- [24] R. Rannacher, On Chorin's projection method for the incompressible Navier-Stokes equations, *Lecture Notes in Mathematics*, Springer, Berlin, (1992), 167-183.
- [25] J. Shen, On pressure stabilization method and projection method for unsteady Navier-Stokes equations, *Advances in Computer Methods for Partial Differential Equations*, IMACS, R. Vichnevetsky, D. Knight, G. Richter (ed.), (1992), 658-662.
- [26] J. Shen, On error estimates of projection methods for the Navier-Stokes equations: second order schemes, *Math. Comp.*, **65** (1996), 1039-1065.
- [27] J.C. Strikwerda, Y.S. Lee, The accuracy of the fractional step method, *SIAM J. Numer. Anal.*, **37**:1(electronic) (1999), 37-47.
- [28] R. Temam, Sur l'approximation de la solution des équations de Navier-Stokes par la méthode des pas fractionnaires ii, *Arch. Rat. Mech. Anal.*, **33** (1969), 377-385.
- [29] R. Temam, *Navier-Stokes Equation: Theory and Numerical Analysis*, North-Holland, Amsterdam, 1984.
- [30] L.J.P. Timmermans, P.D. Mineev, F.N. Van De Vosse, An approximate projection scheme for incompressible flow using spectral elements, *Inter. J. Numer. Meth. Fluids*, **22** (1996), 673-688.
- [31] C.J. Xu, Y.M. Lin, Analysis of iterative methods for the viscous/inviscid coupled problem via a spectral element approximation, *Inter. J Numer. Meth. Fluids*, **32** (2000), 619-646.